EFFECT OF ANTIMONY ON AUSTENITE TRANSFORMATION AND THE METALLIC MATRIX STRUCTURE IN DIFFERENT WALL THICKNESSES OF DUCTILE IRON CASTINGS

Prof. Glavas Z. PhD.[1], Assoc. Prof. Strkalj A. PhD.[1], Janđel J. BSc.[2]
University of Zagreb, Faculty of Metallurgy, Sisak, Croatia [1]
Foundry Ferro-Preis, Čakovec, Croatia [2]

glavaszo@simet.hr

Abstract: *Effects of additions of 0.0039, 0.01, 0.019 and 0.029 wt.% Sb on austenite transformation and the metallic matrix structure in the wall thicknesses of 3, 12, 25, 38, 50, 75 and 100 mm of ductile iron casting containing 2.11 wt.% Si and a low amount of Cu, Sn and Mn were analyzed in this paper. In the examined ductile iron casting without the addition of Sb, the share of pearlite in the metal matrix was decreased and the share of ferrite was increased with increasing wall thickness. The share of pearlite was low. Additions of Sb were increased the share of pearlite in all the walls. Increase of Sb content resulted in increasing the share of pearlite. Almost the same high share of pearlite in the wall thicknesses of 12, 25, 38, 50, 75 and 100 mm was obtained by addition of 0.029 wt. % Sb (varied from 96.00 to 97.61 %). The additions of 0.01, 0.019 and 0.029 wt.% Sb were resulted in a fully pearlitic metallic matrix in the wall thickness of 3 mm. Iron carbides were found in the wall thickness of 3 mm when Sb was added.*

Keywords: DUCTILE IRON CASTING, AUSTENITE TRANSFORMATION, METALLIC MATRIX STRUCTURE, ANTIMONY, MICROSTRUCTURE

1. Introduction

Ductile iron belongs to the family of cast irons containing graphite particles in the microstructure. These particles have a spheroidal (nodular) shape in a ductile iron and are not interconnected. This enables significantly better utilization of the mechanical properties of the metallic matrix than in the case of flake or vermicular shape of graphite particles. Due to these facts, ductile iron has significantly greater mechanical properties than other graphitic cast irons.

Metallic matrix greatly influences the mechanical properties of ductile iron [1 - 4]. Another important factor is the graphite morphology [5 - 8]. In most cases, the metallic matrix is composed of ferrite or pearlite or ferrite + pearlite. Elongation and toughness of ductile iron increase with increasing the share of ferrite. On the other hand, an increase in the share of pearlite results in an increase in tensile strength and yield strength.

Chemical composition, the number and distribution of graphite nodules, and the cooling rate are the most important factors that affect the transformation of austenite and the structure of the metallic matrix of ductile iron [1, 2, 9, 10]. Sn, Cu, Mn, Ni, Cr, etc. are pearlite promoting elements. On the other hand, Si is a ferrite promoter. The share of ferrite in the metallic matrix generally increases with increasing the number of graphite nodules. Increasing the cooling rate increases the share of pearlite and decreases the share of ferrite.

Sb is pearlite promoting element [1, 2, 11 - 13]. Pearlite promoting effectiveness of Sb can be seen from the pearlitic influence factor (P_x) [14, 15]:

$$P_x = 3.0\ (\text{wt.\% Mn}) - 2.65\ (\text{wt.\% Si} - 2.0) + 7.75\ (\text{wt.\% Cu}) + 90\ (\text{wt.\% Sn}) + 357\ (\text{wt.\% Pb}) + 333\ (\text{wt.\% Bi}) + 20.1\ (\text{wt.\% As}) + 9.60\ (\text{wt.\% Cr}) + 71{,}7\ (\text{wt.\% Sb}) \quad (1)$$

Equation 1 shows that the Sb is considerably more powerful pearlite promoting element than Cu, which is most commonly used for increasing the share of pearlite in ductile iron. During solidification Sb is adsorbed on the surface of graphite nodules and forms a barrier that prevents the diffusion of carbon atoms from austenite to nodules during the cooling after solidification [1, 11, 16]. The high content of carbon remains in austenite. This results in the transformation of austenite to pearlite.

When we use Sb in ductile iron, we have to consider that it also affects the graphite morphology. The Sb content above 0.004 wt.% hinders the formation of spheroidal graphite, particularly in the thick walls [2]. It segregates to the intercellular regions where promotes the formation of very harmful intercellular flake graphite [1, 2, 17, 18]. Studies have shown that the detrimental effect of Sb on the graphite morphology can be neutralized by adding appropriate amount of RE elements [14, 18 - 20].

Real castings in most cases do not have a uniform thickness. The cooling rates of certain segments of casting vary due to differences in thickness. In this case the casting will not have a uniform structure of the metallic matrix. This means that the casting will not have the same properties in all areas. Uniform pearlitic metallic matrix is difficult to achieve in the ductile iron casting containing a thin, medium-thick and thick walls. The thick walls often contain a higher share of ferrite. It would be useful to investigate whether Sb can reduce variations in the structure of the metallic matrix in such castings. This paper deals with the influence of various Sb contents on austenite transformation and the structure of the metallic matrix in low-silicon ductile iron casting containing a thin, medium-thick and thick walls.

2. Experimental

Special low-manganese pig iron (50 wt.%), steel scrap (20 wt.%) and ductile iron returns (30 wt.%) were used for the production of the base iron. Melting was performed in a medium-frequency coreless induction furnace. Preconditioning of the base iron was carried out using commercial preconditioner containing 63 to 69 wt.% Si, 3 to 5 wt.% Al, 0.6 to 1.9 wt.% Ca, and 3 to 5 wt.% Zr. The addition of preconditioner was 0.1 wt.%. The Si content in the base iron was adjusted to achieve Si content between 2.0 and 2.2 wt.% in ductile iron melt.

FeSiMg treatment alloy containing 29 wt.% Mg, 42 wt.% Si, 1.4 wt.% Ca, 0.9 wt.% Al, 0.2 wt.% La and 0.5 wt.% Ce was used for graphite spheroidization, i.e., nodularization in the Cored wire process. The first step of inoculation was performed at the same time by the addition of the commercial inoculant containing 67 to 72 wt.% Si, 1.5 wt.% Ca, 1.9 wt.% Al, and 2.2 wt.% Ba. The addition of inoculant was 0.5 wt.%.

The step wedge test block (SWTB) consisted of seven walls with the following thicknesses: 3, 12, 25, 38, 50, 75 and 100 mm (Fig. 1). Five step wedge test blocks were casted in green sand molds. The second step of inoculation was performed during the pouring of the ductile iron melt into the molds. Commercial inoculant containing 70 to 76 wt.% Si, 0.75 to 1.25 wt.% Ca, 0.75 to 1.25 wt.% Al and 1.5 to 2 wt.% Ce was added to the melt stream in the amount of 0.2 wt.%. The first SWTB was casted without the addition of Sb. Pure Sb (99.99 wt.%) was added in second, third, fourth and fifth SWTB along with inoculant. Targeted Sb contents are shown in Tab. 1.

Samples for determining the contents of C, Si, Mn, P, S, Cr, Mo, Ni, Cu V, W and Mg were taken immediately before pouring

the ductile iron melt into molds. The contents of these elements were determined by optical emission spectrometry (OES). Samples for determining the contents of Sb, Ce, La, Nd, Pr, Gd, Sm, Y, Sn, Ti, Cd, Bi, Zr, Nb, Ca, Co, As, Pb and Al were cut from the step wedge test blocks. The contents of these elements were determined by inductively coupled plasma mass spectroscopy (ICP-MS).

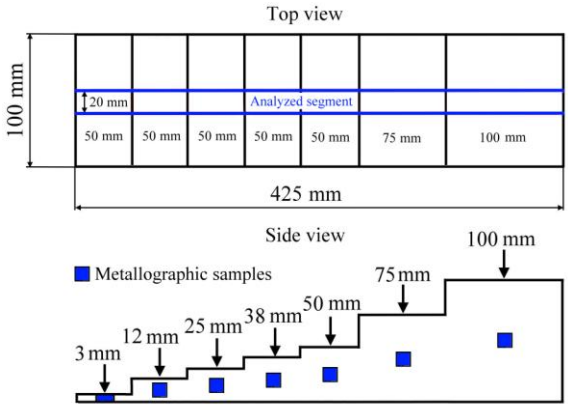

Fig. 1 *Schematic show of the step wedge test blocks and places where samples for metallographic analysis were taken.*

Table 1: *Additions of inoculant in melt stream during pouring into the mold and the targeted Sb contents.*

Step wedge test block (SWTB)	Additions of inoculant in melt stream, wt. %	Targeted Sb contents, wt. %
SWTB 1	0.2	-
SWTB 2	0.2	0.005
SWTB 3	0.2	0.01
SWTB 4	0.2	0.02
SWTB 5	0.2	0.03

Fig. 1 shows places where samples for metallographic analysis were taken. Light metallographic microscope with a digital camera and the image analysis system was used for the analysis of microstructure of samples.

3. Results and discussion

The chemical compositions of step wedge test blocks are shown in Tab. 2.

Table 2: *Chemical composition of examined step wedge test blocks (* P_x - pearlitic influence factor (defined by the Eq. (1)).*

Step wedge test block (SWTB)	Chemical composition, wt.%				P_x^*
	Elements	Ce	Al	Sb	
SWTB 1	C-3.55; Si-2.11, Mn-0.098; P-0.035; S-0.012; Mg-0.048; Cu-0.018; Cr-0.029; Mo-0.002; Ni-0.016; V-0.01; W-0.0015; Sn-0.0055; La-0.00045; Pr-0.0000038; Nd-0.000012; Sm-0.0000017; Gd-0.000003; Bi-0.000011; Pb-0.00052; As-0.00015; Ti-0.0169; Nb-0.0039; Zr-0.0029; Y-0.000014; Ca-0.0048;Co-0.016; Cd-0.000017	0.0025	0.014	0.00042	1.14
SWTB 2		0.0028	0.018	0.0039	1.39
SWTB 3		0.0029	0.016	0.01	1.82
SWTB 4		0.0034	0.016	0.019	2.47
SWTB 5		0.003	0.019	0.029	3.19

It can be seen that the targeted Sb contents and targeted Si content were achieved. Yield of Sb was varied from 69.6 to 95.8 %. Low Si content was chosen because it adversely affects the graphite morphology in the thick walls and promotes the formation of ferrite. RE elements (Ce and La) were added through the inoculant and FeSiMg treatment alloy because these elements neutralize the harmful (antinodularizing) effect of Sb on the morphology of graphite. In addition, these elements increase the nodule count in thin walls, which is important for preventing the formation of carbides in these walls. The data in Tab. 2 show that the content of carbide promoting elements was low. With the exception of Sb, the content of other pearlite promoting elements was low. Pearlitic influence factor P_x (defined by the Eq. [1]) significantly increases with increasing Sb content.

The obtained results of metallographic analysis indicate that the wall thickness and the Sb content have a very significant effect on the structure of the metallic matrix in ductile iron castings (Figs. 2 and 3). In SWTB 1, where Sb was not added, the share of ferrite in the metallic matrix increases, and the share of pearlite decreases with increasing wall thickness due to decrease in the cooling rate. The share of pearlite is low (varies from 11.92 % (in the wall thickness of 100 mm) to 32.95 % (in the wall thickness of 3mm)). Addition of Sb increased the share of pearlite in all the walls (SWTB 2 – 5). The share of pearlite increases with increasing Sb content.

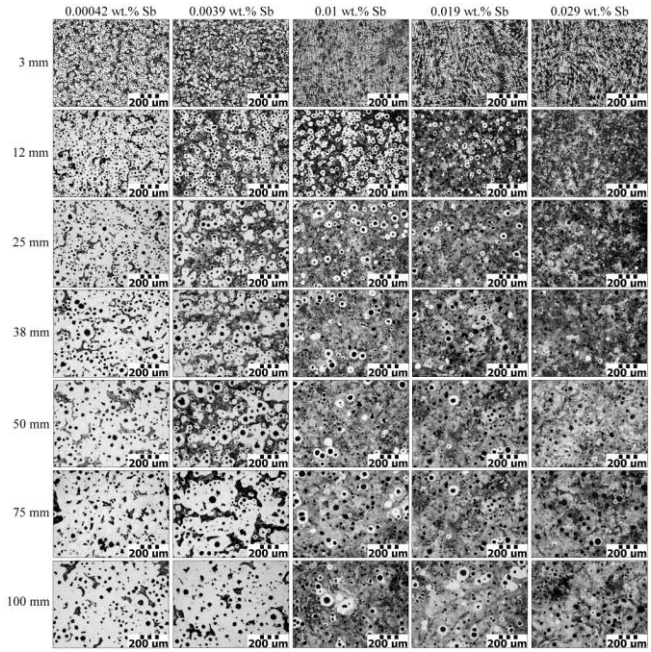

Fig. 2 *Optical micrographs of the central part of the wall thicknesses of 3, 12, 25, 38, 50, 75 and 100 mm at various Sb contents (etched in Nital).*

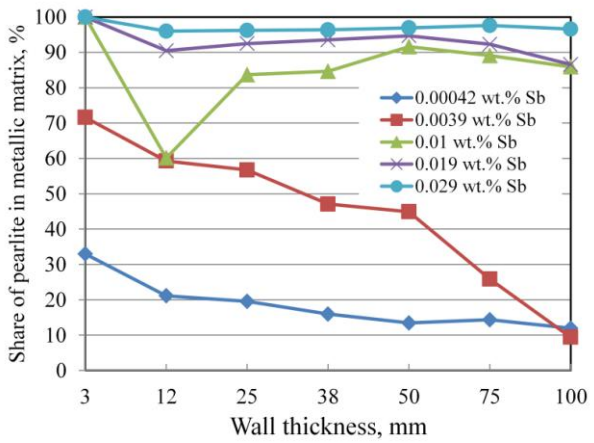

Fig. 3 *Effect of Sb addition on the share of pearlite in the metallic matrix of the wall thickness of 3, 12, 25, 38, 50, 75 and 100 mm.*

Addition of only 0.0039 wt.% Sb in SWTB 2 increased the share of pearlite in all the walls compared to SWTB 1 (Figs. 2 and 3). The effect is more pronounced in the wall thicknesses of 3, 12, 25, 38 and 50 mm. The share of pearlite is not significantly increased in the walls thicknesses of 75 and 100 mm. It is obvious that the thicker walls require a higher Sb addition due to very slow cooling. Iron carbides are present in the wall thickness of 3 mm. Since the wall thickness of 3 mm in SWTB 1 does not contain carbides, obtained results indicate that Sb promotes the formation of iron carbides in very thin walls when the Si content is low because it lowers the stable and metastable eutectic temperatures.

Increase of Sb content to 0.01 wt.% (SWTB 3) resulted in a further increase in the share of pearlite in all the walls (Figs. 2 and 3). The variations in the share of pearlite between the walls are significantly lower than in SWTB 1 and SWTB 2. Fully pearlitic metallic matrix is obtained in the wall thickness of 3 mm. The share of pearlite in the wall thicknesses of 25, 38, 50, 75 and 100 mm is greater than 80 % (varies from 83.67 % to 91.59 % depending on the wall thickness and nodule count). Nodule count increased with decreasing wall thickness and influenced the formation of pearlite. Increasing the share of pearlite is slightly lower in the wall thickness of 12 mm due to the high nodule count. It is obvious that a high nodule count facilitates the formation of ferrite and hinders the formation of pearlite. Therefore, required addition of Sb for obtaining pearlitic metallic matrix increases with an increase in the nodule count. The share of iron carbides is greater than in SWTB 2 due to higher Sb content.

The share of pearlite greater than 90 % was obtained in the wall thicknesses of 12, 25, 38, 50 and 75 mm in SWTB 4 by the addition of 0.019 wt.% Sb (Figs. 2 and 3). In the wall thickness of 100 mm, the share of pearlite is slightly lower than in the other walls. Fully pearlitic metallic matrix is obtained in the wall thickness of 3 mm. The variations in the share of pearlite between the walls are further decreased. The share of iron carbides in the wall thickness of 3 mm is further increased due to increase in Sb content.

Very uniform pearlitic metallic matrix was obtained in the SWTB 5 containing 0.029 wt.% Sb (Figs. 2 and 3). Fully pearlitic metallic matrix is obtained in the wall thickness of 3 mm. Almost the same share of pearlite was obtained in the wall thicknesses of 12, 25, 38, 50, 75 and 100 mm (varies from 96.00 to 97.61 %). Ferrite is present only in a narrow area around the nodules. It is obvious that sufficiently high Sb content eliminates the influence of the cooling rate and the nodule count on the share of ferrite in the metallic matrix. Due to higher Sb content, share of iron carbides in the wall thickness of 3 mm is further increased.

Fig. 2 shows that all Sb additions had a positive effect on the graphite morphology, except in the wall thickness of 3 mm. The effect is more pronounced in the thick walls. Nodularity and nodule count were significantly increased in the wall thicknesses of 50, 75 and 100 mm. This indicates that the content of RE elements (Ce + La) was sufficient considering the added amounts of Sb (wt.% Ce + wt.% La was varied from 0.00325 to 0.00385 wt.%). RE elements react with Sb and neutralize its harmful effect on the graphite morphology [18, 21, 22]. Nucleation potential of the melt is improved at the same time, because formed intermetallic compounds act as nucleation sites for graphite [18, 21, 22].

4. Conclusions

Obtained results show that the Sb is a very effective element for increasing the share of pearlite in the metallic matrix of thin, medium-thick and thick walls of ductile iron castings. Required addition of Sb for obtaining pearlitic metallic matrix increases with increasing wall thickness and nodule count. Sb reduces variations in the structure of the metallic matrix of ductile iron castings. It allows to obtain a uniform pearlitic metallic matrix in ductile iron castings containing a thin, medium-thick and thick walls. This reduces the variation of mechanical properties in the casting.

RE elements (Ce and La) neutralize the deleterious effect of Sb on the graphite morphology in ductile iron castings. Moreover, when Sb is added together with the appropriate amount of RE elements, it increases the nodule count and nodularity in medium thick and thick walls. This positive effect of Sb on the graphite morphology is significantly more pronounced in the thick walls.

In addition to the identified positive effects of Sb, one negative effect was also found. Already very low Sb content promotes the formation of iron carbides in a very thin wall (3 mm) when the Si content is low.

5. References

[1] M. Gagné, The Sorelmetal Book of Ductile Iron, Rio Tinto Iron & Titanium, Montreal, Canada, 2004.

[2] …, Ductile Iron Handbook, ed. W. A. Henning, J. Mercer, American Foundry Society, Inc., Illinois, 2010.

[3] R.A. Gonzaga, Influence of Ferrite and Pearlite Content on Mechanical Properties of Ductile Cast Irons, Materials Science and Engineering A 567(2013), 1 – 8.

[4] R.A. Gonzaga, P. Martínez Landa, A. Perez, P. Villanueva, Mechanical Properties Dependency of the Pearlite Content of Ductile Irons, Journal of Achievements in Materials and Manufacturing Engineering 33(2009) 2, 150 – 158.

[5] P. Ferro, A. Fabrizi, R. Cervo, C. Carollo, Effect of Inoculants Containing Rare Earth Metals and Bismuth on Microstructure and Mechanical Properties of Heavy-Section Near-Eutectic Ductile Iron Castings, Journal of Materials Processing Technology 213(2013) 9, 1601 – 1608.

[6] P. Ferro, P. Lazzarin, F. Berto, Fatigue Properties of Ductile Iron Containing Chunky Graphite, Materials Science and Engineering A 554(2012), 122 – 128.

[7] I. Riposan, M. Chisamera, A. Stan, Control of Surface Graphite Degeneration in Ductile Iron for Windmill Applications, International Journal of Metalcasting 7(2013) 1, 9 – 20.

[8] C. Labrecque, P.M. Cabanne, Low Temperature Impact Strength of Heavy Section Ductile Iron Castings: Effect of Microstructure and Chemical Composition, China Foundry 8(2011) 1, 66 – 73.

[9] X. Guo, D.M. Stefanescu, Solid Phase Transformation in Ductile Iron – A Benchmark for Computational Simulation of Microstructure, AFS Transactions 105(1997), 533 - 543.

[10] D. Venugopalan, A Kinetic Model of the $\gamma \rightarrow \alpha$ + Gr Eutectoid Transformation in Spheroidal Graphite Cast Irons, Metallurgical Transactions A 21(1990) 4, 913 - 918.

[11] M.M. Mourad, S. El-Hadad, M.M Ibrahim, A.A. Nofal, Effect of Processing Parameters on the Mechanical Properties of Heavy Section Ductile Iron, Journal of Metallurgy, vol. 2015, Article ID 931535, 11 pages, 2015. doi:10.1155/2015/931535.

[12] M. Wessén, I.L. Svensson, R. Aagaard, Influence of Antimony on Microstructure and Mechanical Properties in Thick- walled Ductile Iron Castings, International Journal of Cast Metals Research 16(2003) 1 - 3, 119 – 124.

[13] L. Zhe, C. Weiping, D. Yu, Influence of Cooling Rate and Antimony Content on Graphite Morphology and Mechanical Properties of a Ductile Iron, China Foundry 9(2012) 2, 114 – 118.

[14] I. Riposan, M. Chisamera, S. Stan, Performance of Heavy Ductile Iron Castings for Windmills, China Foundry 7(2010) 2, 163 - 170.

[15] I. Riposan, M. Chisamera, S. Stan, Influencing Factors on As-cast and Heat Treated 400-18 Ductile Iron Grade Characteristics, China Foundry 4(2007) 4, 300 - 303.

[16] W.C. Johnson, B.V. Kovacs, The Effect of Additives on the Eutectoid Transformation of Ductile Iron, Metallurgical Transactions A 9(1978) 2, 219 - 229.

[17] Z. Jiyang, Colour Metallography of Cast Iron, Chapter 3, Spheroidal Graphite Cast Iron (II), China Foundry 7(2010) 2, 183 – 198.

[18] A. Javaid , C.R. Loper, Jr.: Production of Heavy-section Ductile Cast Iron, AFS Transactions 103(1995), 135 - 150.

[19] I. Riposan, M. Chisamera, V. Uta, S. Stan, The Importance of Rare Earth Contribution From Nodulizing Alloys and Their Subsequent Effect on the Inoculation of Ductile Iron, International Journal of Metalcasting 8(2014) 2, 65 – 80.

[20] Z. Glavas, A. Strkalj, K. Maldini, Effects of Antimony and Wall Thickness on Graphite Morphology in Ductile Iron Castings, Metallurgical and Materials Transactions B 47(2016) 4, 2487 - 2497.

[21] E.N. Pan, C.Y. Chen, Effects of Bi and Sb on Graphite Structure of Heavy-Section Ductile Cast Iron, ASF Transaction 104(1996), 845 – 858.

[22] Z. Jiyang, Colour Metallography of Cast Iron, Chapter 3, Spheroidal Graphite Cast Iron (I), China Foundry 7(2010) 1, 76 - 88.